

1 **SUPPLEMENTAL METHODS**

2 **Cell clustering and cell type annotation**

3 The R package Seurat (v3.1.2) was used to cluster the cells in the merged matrix ¹. Cells with less
4 than 500 transcripts or 100 genes, or more than 10% of mitochondrial expression were first filtered
5 out as low-quality cells. The NormalizeData was used to normalize the expression level for each
6 cell with default parameters. The FindVariableFeatures function was used to select variable genes
7 with default parameters. The FindIntegrationAnchors and IntegrateData functions were used to
8 integrate the samples prepared using different 10X Chromium chemistries. The ScaleData function
9 was used to scale and center the counts in the dataset. Principal component analysis (PCA) was
10 performed on the variable genes, and the first 20 PCs were used for cell clustering and Uniform
11 Manifold Approximation and Projection (UMAP) dimensional reduction. The clusters were
12 obtained using the FindNeighbors and FindClusters functions with the resolution set to 0.5. The
13 cluster marker genes were found using the FindAllMarkers function. The cell types were annotated
14 by overlapping the cluster markers with the canonical cell type signature genes. To calculate the
15 disease composition based on cell type, the number of cells for each cell type from each disease
16 condition were counted. The counts were then divided by the total number of cells for each disease
17 condition and scaled to 100 percent for each cell type. Differential expression analyses between
18 NS and HS or any two groups of cells were carried out using the FindMarkers function.

19

20 **Cell type subclustering**

21 Subclustering was performed on the abundant cell types. The same functions described above were
22 used to obtain the subclusters. Subclusters that were defined exclusively by mitochondrial gene
23 expression, indicating low quality, were removed from further analysis. The subtypes were
24 annotated by overlapping the marker genes for the subclusters with the canonical subtype signature

25 genes. Ingenuity pathway analysis was applied to the differentially expressed genes to determine
26 the canonical pathways and the potential upstream regulators. The upstream regulators with an
27 activation z score ≥ 2 were considered significantly activated. The module scores were calculated
28 using the AddModuleScore function on the genes induced by the intended cytokine from bulk
29 RNA-seq analysis. To obtain the cytokine induced genes, healthy donor derived keratinocytes and
30 fibroblasts were cultured and stimulated with respective cytokine for 8 hours ². Bulk RNA-seq and
31 differential expression analysis (DESeq2) were performed between the cytokine stimulated and
32 the control keratinocytes or fibroblasts. Genes with adjusted p-value < 0.05 that are also highly
33 expressed in the cytokine stimulated keratinocytes were considered cytokine induced genes. The
34 module scores for the upstream regulators were calculated on the target gene lists from the
35 Ingenuity Pathway Analysis software.

36

37 **Ligand receptor interaction analysis**

38 CellphoneDB (v2.0.0) was applied for ligand receptor analysis ³. The Seurat normalized counts
39 and subcluster annotation for each cell were input into cellphoneDB to determine the potential
40 ligand receptor pairs. Pairs with p value > 0.05 were filtered out from further analysis. The
41 subclusters were divided into NS specific subcluster (with NS composition $> 70\%$), HS specific
42 subcluster (with HS composition $> 70\%$) and mixed subcluster. CellphoneDB was then run on the
43 NS cells from the NS specific subclusters and HS cells from the HS specific subclusters. The pairs
44 from the subclusters for the same cell type were merged to find ligand-receptor pairs between the
45 major cell types. The pairs with higher interaction score in HS were plotted. The connectome web
46 was plotted using the R package igraph.

47

48 **Pseudotime trajectory construction**

49 Pseudotime trajectory was constructed using the R package Monocle ⁴. The raw counts for cells
50 were extracted from the Seurat analysis and normalized by the estimateSizeFactors and
51 estimateDispersions functions with the default parameters. Genes with average expression larger
52 than 0.5 and detected in more than 10 cells were retained for further analysis. Variable genes were
53 determined by the differentialGeneTest function with a model against the Seurat subcluster
54 identities for the subtype identities of the NS or HS cell types. The orders of the cells were
55 determined by the orderCells function, and the trajectory was constructed by the reduceDimension
56 function with default parameters. The heatmap showing specific genes along pseudotime was
57 plotted using the plot_pseudotime_heatmap function. Differential expression between pseudo-
58 time states was carried out using the Seurat function FindMarkers. Ingenuity Pathway Analysis
59 was used to determine the upstream regulators for the DEGs.

60

61 **Spatial transcriptomics library preparation**

62 Four lesional HS skin samples were frozen in OCT medium and stored at -80°C until sectioning.
63 Optimization of tissue permeabilization was performed on 20-µm-thick sections using Visium
64 Spatial Tissue Optimization Reagents Kit (10X Genomics, Pleasanton, CA, USA), which
65 established an optimal permeabilization time to be 24 minutes. Samples were mounted onto a Gene
66 Expression slide (10X Genomics), fixed in ice-cold methanol, stained with hematoxylin and eosin,
67 and scanned under a microscope (Keyence, Itasca, IL, USA). Tissue permeabilization was
68 performed to release the poly-A mRNA for capture by the poly(dT) primers that are precoated on
69 the slide and include an Illumina TruSeq Read, spatial barcode, and unique molecular identifier
70 (UMI). Visium Spatial Gene Expression Reagent Kit (10X Genomics) was used for reverse

71 transcription to produce spatially barcoded full-length cDNA and for second strand synthesis
72 followed by denaturation to allow a transfer of the cDNA from the slide into a tube for
73 amplification and library construction. Visium Spatial Single Cell 3' Gene Expression libraries
74 consisting of Illumina paired-end sequences flanked with P5/P7 were constructed after enzymatic
75 fragmentation, size selection, end repair, A-tailing, adaptor ligation, and PCR. Dual Index Kit TT
76 Set A (10X Genomics) was used to add unique i7 and i5 sample indexes and generate TruSeq Read
77 1 for sequencing the spatial barcode and UMI and TruSeq Read 2 for sequencing the cDNA insert,
78 respectively. Libraries were sequenced on the Illumina NovaSeq 6000 sequencer to generate 150
79 bp paired end reads.

80

81 **Spatial transcriptomics data analysis**

82 After sequencing, the reads were aligned to the human genome (hg38), and the expression matrix
83 was extracted using the spaceranger pipeline. Seurat was then used to analyze the expression
84 matrix. Specifically, the SCTransform function was used to scale the data and find variable genes
85 with default parameters. PCA and UMAP were applied for dimensional reduction. The
86 FindTransferAnchors function was used to find a set of anchors between the scRNA-seq data and
87 spatial-seq data, which were then transferred from the scRNA-seq to the spatial-seq data using the
88 TransferData function. The major cell types obtained in the scRNA-seq data were used to annotate
89 the spatial-seq data. The predicted cell type composition for each spot was then used to cluster the
90 spots by the k-means algorithm. The clusters were annotated based on the average cell type
91 prediction score across all the spots in the cluster.

92

93

94 **Immunohistochemistry and trichrome staining**

95 Formalin-fixed embedded human tissues were sectioned and heated at 65 °C for 5 minutes,
96 deparaffinized, and rehydrated. Slides were placed in pH9 antigen retrieval buffer and heated at
97 125 °C for 30 seconds in a pressure cooker water bath. After cooling, slides were treated with 3%
98 H₂O₂ (5 minutes) and blocked using 10% goat serum or horse serum (30 minutes). Overnight
99 incubation (4°C) was then performed using anti-human primary antibody. Antibodies used were:
100 CD3 (UM500048, 1:300), CD20 (AB9475, 1:20), CD11c (ab52632, 2µg/ml), CD31 (ab28364,
101 1:25), CD138 (LS-B9360, 1:40), KRT16 (LS-B7609, 2µg/ml), NE (MAB91671, 10µg/ml),
102 ACTA2 (ab5694, 1:100), CD207 (PA5-82422, 1:200), CLEC9A (55451-I-AP, 1:70), LAMP3
103 (PA5-84069, 1:50), CD303 (Hpa029432, 1:20), CLEC10A (TA810180, 1:150), CD163 (MA5-
104 11458, 1:25), LSP1 (LS-B16949-50, 2µg/ml) SFRP2 (LS-C794043, 1:300), SFRP4 (LS-C408100,
105 1:250), RAMP1 (AB203282, 1:200), COL11A1 (PA5-68410, 1:300), and CXCL13 (LS-C490370,
106 2µg/ml), YAP1 (ab205270, 1:2000), TAZ (HPA007415, 1:100), TEAD1 (#12292,1:100), TEAD2
107 (ab196669, 1:50), TEAD4 (H00007004, 3ug/ml). Slides were then washed, treated with secondary
108 antibody (30 minutes), peroxidase (30 minutes) and diaminobenzidine substrate. Counterstain with
109 Hematoxylin and dehydration was performed, and slides were mounted and viewed under the
110 microscope. In addition, slides were stained with Masson's trichrome stain as previously
111 described.

112

113 **Immunofluorescence staining**

114 Antigen retrieval was performed as described above. Formalin-fixed embedded human tissues
115 were sectioned and heated at 65 °C for 30 minutes, deparaffinized, and rehydrated. Slides were
116 subsequently blocked and incubated with primary rabbit and mouse anti-human antibodies.

117 Primary rabbit antibodies were used ACTA2 (ab5694, 1:100), CD31 (ab28364, 1:25), LYVE1
118 (ab33682, 5µg/ml), CXCL13 (PA5-47035, 5µg/ml). Primary mouse antibodies used: CD31
119 (ab9498, 10µg/ml), HLA-DR (ab20181, 2µg/ml), CD3 (UM500048, 1:150), vimentin (AB92547,
120 1:200). Appropriate antibodies were co-incubated overnight at 4°C. Appropriate isotype control
121 antibodies: rabbit IgG (ab172730), mouse IgG1 (ab 280974) both from Abcam, IgG2ak (14-4724-
122 82) from Invitrogen, were stained in parallel with each set of the slides mentioned above. Slides
123 were then washed three times for 5 min each with phosphate-buffered saline/ Tween 20 (PBST).
124 All slides were then incubated with secondary antibodies fluorochrome-conjugated Alexa Fluor
125 594 conjugated anti-rabbit IgG (711-585-152) and Alexa Fluor 488 conjugated anti-mouse IgG
126 (715-545-151) from Jackson Immuno Research. After 30 minutes coincubation, slides were
127 washed three times for 5 min each with PBST. Mounted in an Prolong Dimond antifade with DAPI
128 (Invitrogen). Photomicrographs were taken on Zeiss fluorescence microscope.

129

130 **REFERENCES**

- 131 1. Butler, A., Hoffman, P., Smibert, P., Papalexi, E. & Satija, R. Integrating single-cell
132 transcriptomic data across different conditions, technologies, and species. *Nat Biotechnol* **36**,
133 411–420 (2018).
- 134 2. Billi, A. C. *et al.* Nonlesional lupus skin contributes to inflammatory education of myeloid
135 cells and primes for cutaneous inflammation. *Sci Transl Med* **14**, eabn2263 (2022).
- 136 3. Efremova, M., Vento-Tormo, M., Teichmann, S. A. & Vento-Tormo, R. CellPhoneDB:
137 inferring cell-cell communication from combined expression of multi-subunit ligand-receptor
138 complexes. *Nat Protoc* **15**, 1484–1506 (2020).

139 4. Trapnell, C. *et al.* The dynamics and regulators of cell fate decisions are revealed by
140 pseudotemporal ordering of single cells. *Nat Biotechnol* **32**, 381–386 (2014).

141

142

143 **SUPPLEMENTAL TABLES**

144 **Supplemental Table 1. Patient characteristics**

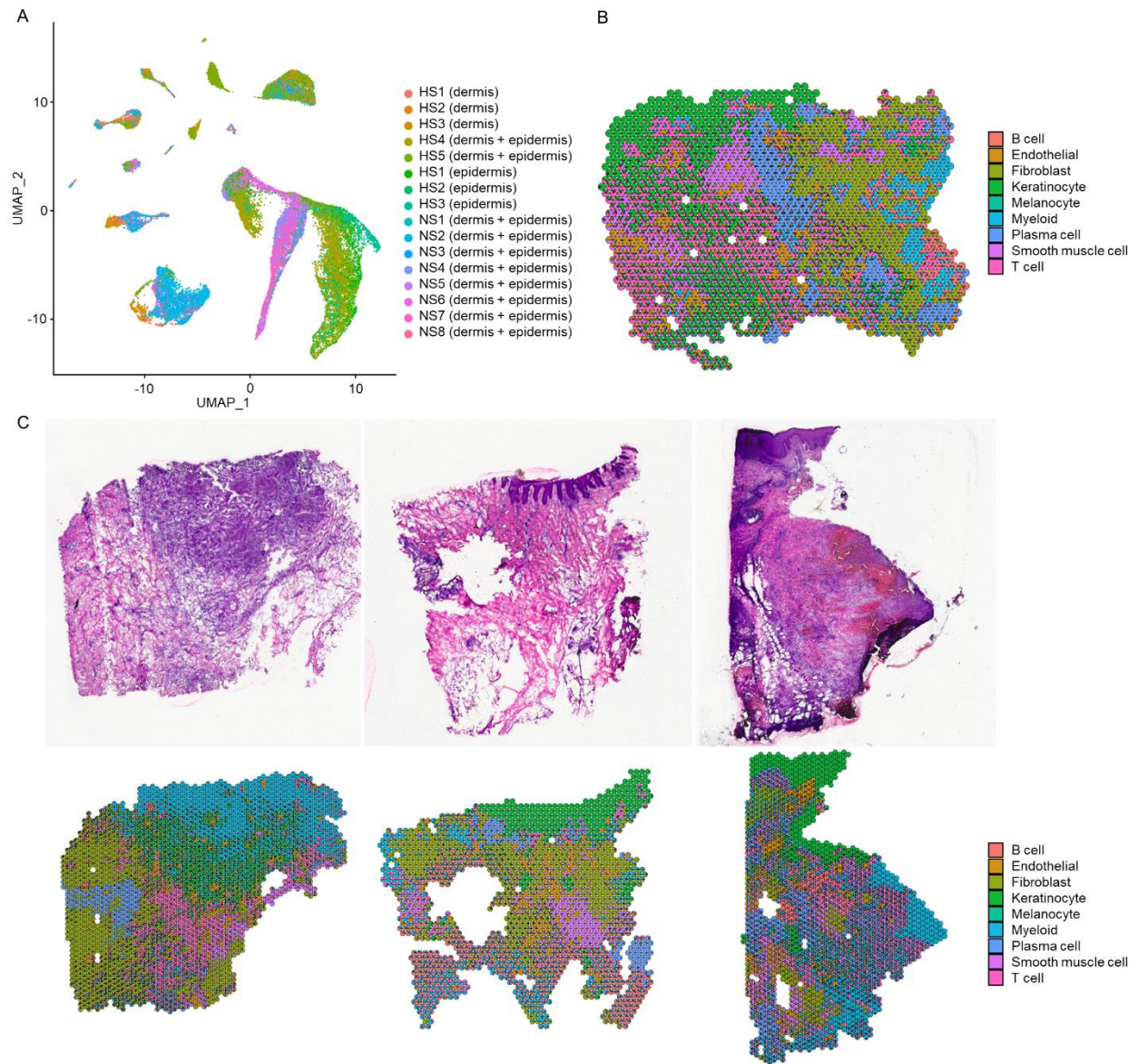
145

	HS patients	
	n=5	
Sex		
Female, <i>n (%)</i>	3	(60)
Male, <i>n (%)</i>	2	(40)
Age in years, mean ±SD	42.22	±14.24
BMI, mean ±SD	28.95	±5.34
Disease duration in years, mean ±SD	20.00	±9.00
Current or ex-smokers, <i>n (%)</i>	5	(100)
Hurley stage		
Hurley stage II, <i>n (%)</i>	1	(20)
Hurley stage III, <i>n (%)</i>	4	(80)
Anatomical location sampled		
Groin, <i>n (%)</i>	4	(80)
Buttock, <i>n (%)</i>	1	(20)

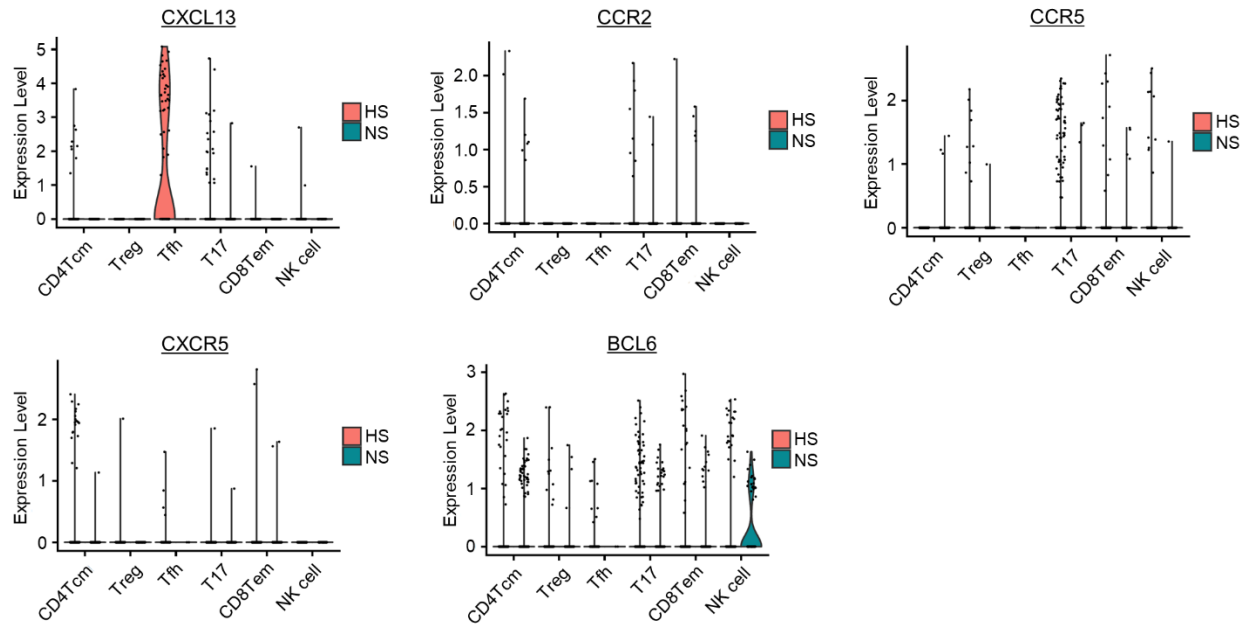
146 HS, hidradenitis suppurativa; SD, standard deviation; BMI, body mass index

147

SUPPLEMENTAL FIGURES



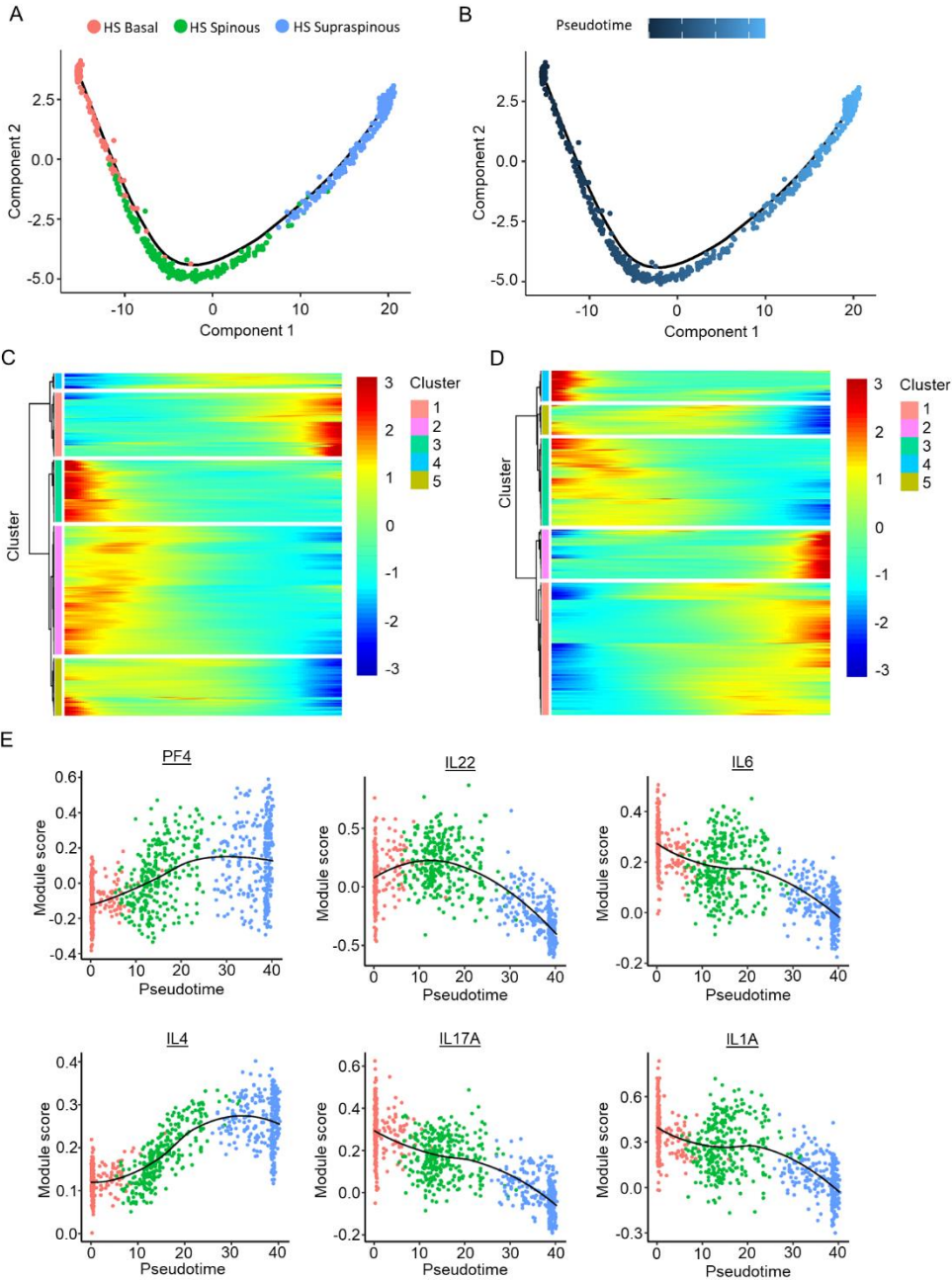
148 **Figure S1. Cell composition and spatial transcriptomics of cell types in three more HS samples.**
 149 (A) UMAP plot showing the cells colored by sequencing libraries. (B) Scatter pie plot showing the cell type
 150 composition of the HS spatial-seq sample. Each spot is represented as a pie chart showing the relative proportion of
 151 the cell types. (C) Spatial transcriptomics for the other three other HS samples. Top panel: H & E staining of the
 152 biopsy used for spatial transcriptomics; bottom panel: scatter pie plot showing the cell type composition.



155
 156
 157
 158

Figure S3. Expression of Tfh and Tph lineage makers among T cells.

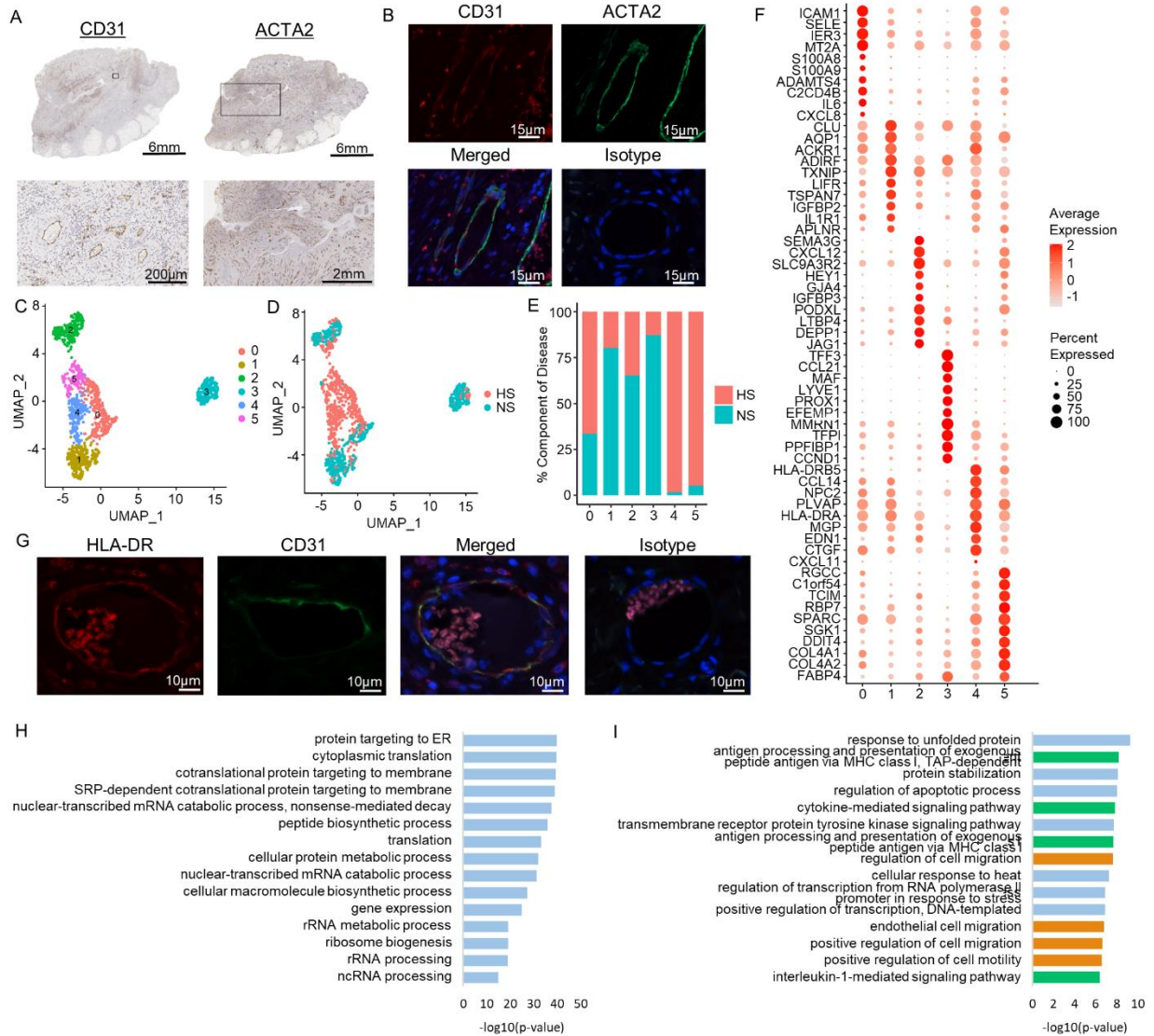
Violin plots showing the expression of genes split by T cell subcluster. Each dot represents the gene's expression in a single T cell.



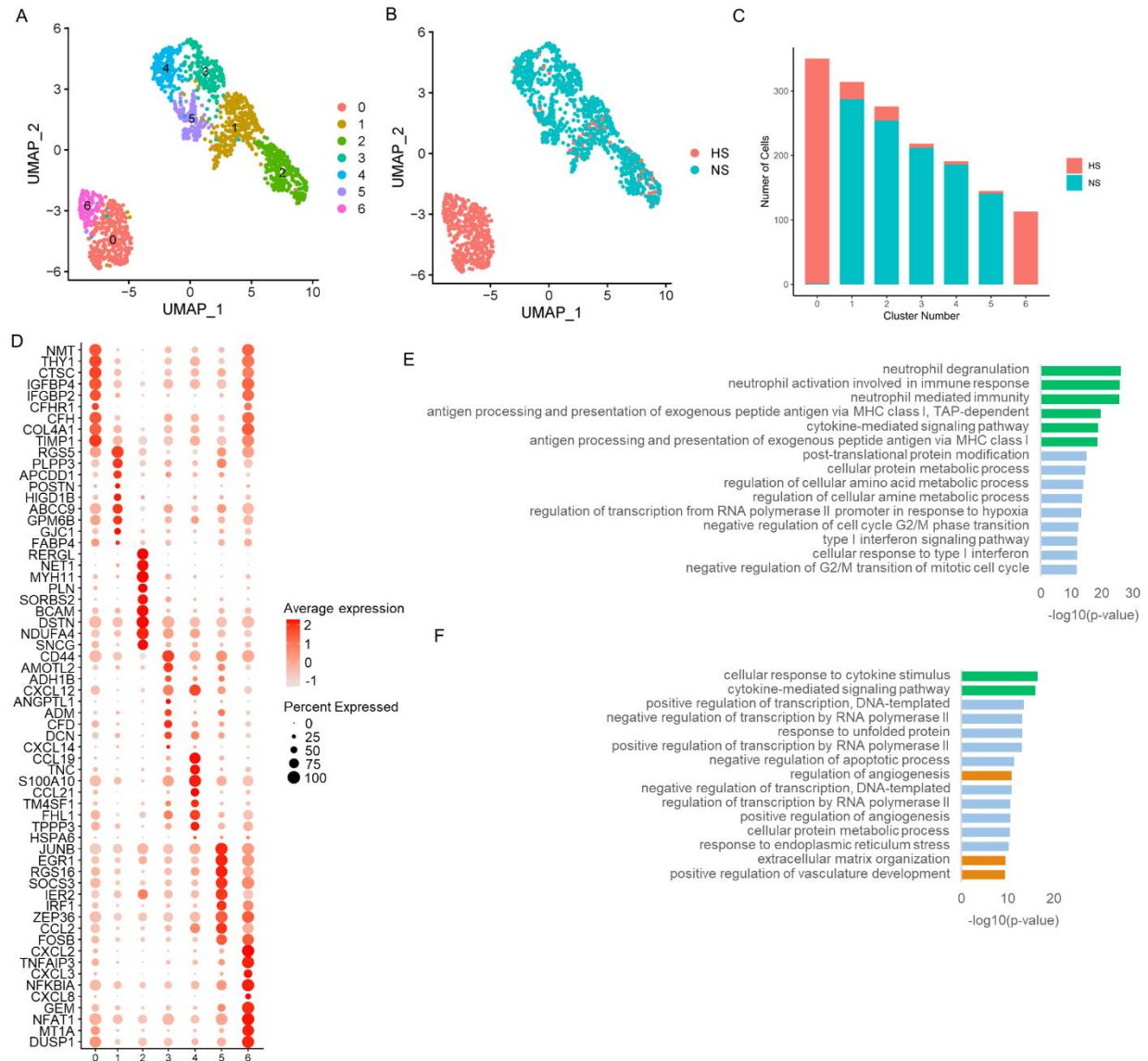
159
 160
 161
 162
 163
 164
 165

Figure S4. Pseudotime trajectory for NS keratinocytes.

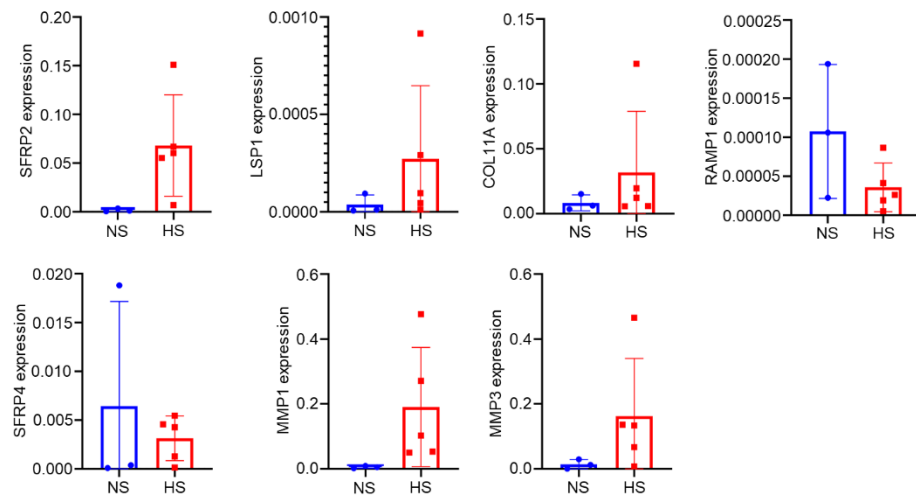
(A) Pseudotime trajectory colored by the subtype identity of NS keratinocytes. (B) Pseudotime trajectory colored by the pseudotime; dark blue representing early, light blue representing late. (C) Heatmap showing the five expression patterns of variable genes along the pseudotime of the NS keratinocytes (D) Scatter plot showing the correlation between HS-derives keratinocyte pseudotimes and module scores for PF4 and IL4. The color represents the pseudotime subtype identity of the cell.



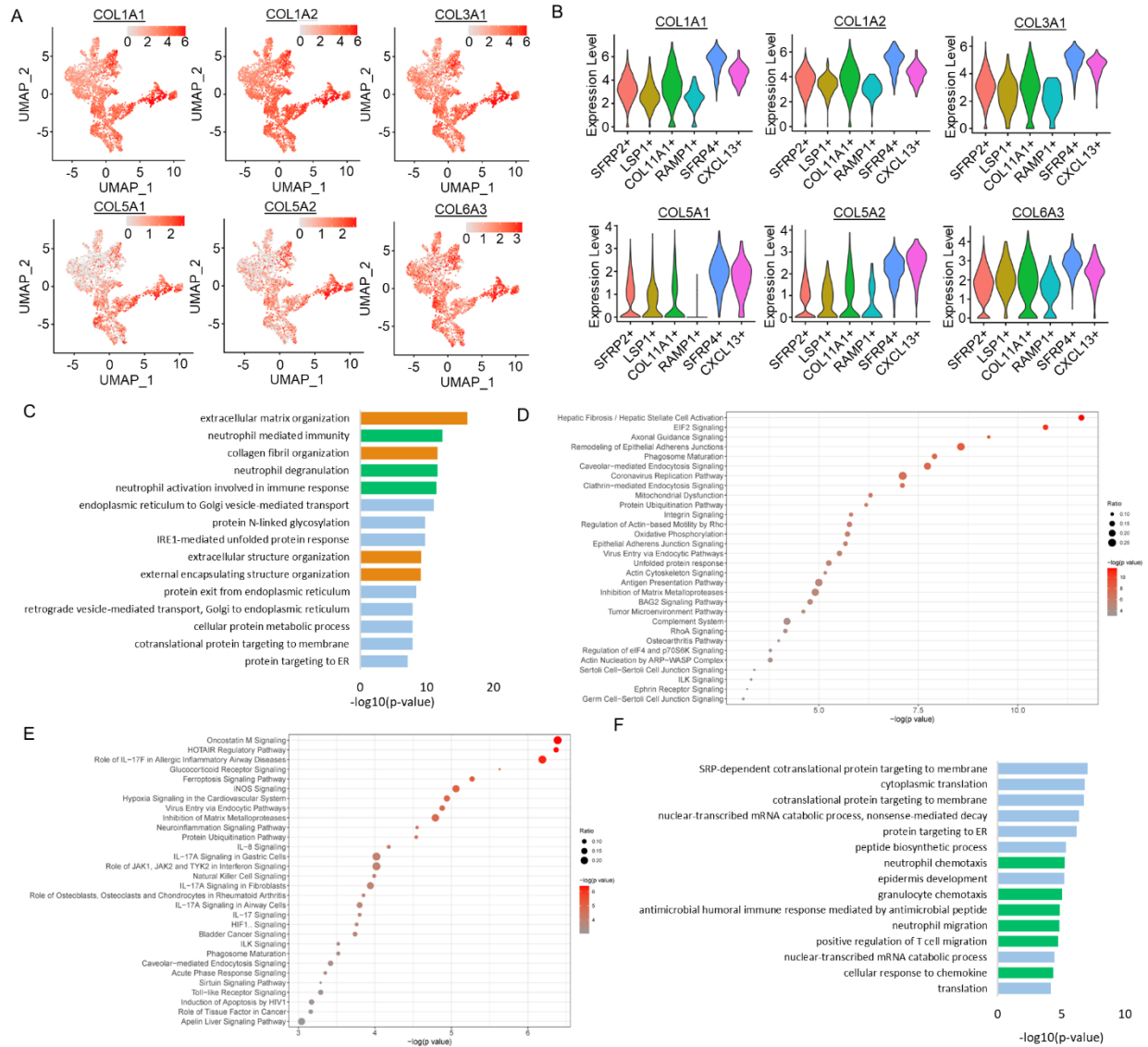
166 **Figure S5. Immunologically active endothelial cell proliferation in HS lesional skin.**
 167 Immunohistochemistry (A) and immunofluorescence (B) showing the prominent neovascularization in HS lesional
 168 skin. ACTA2; smooth muscle cells, CD31; endothelial cells. (C) UMAP plot showing 1,352 endothelial cells colored
 169 by subcluster. (D) UMAP plot showing the cells colored by disease conditions. HS: hidradenitis suppurativa; NS:
 170 normal/healthy skin. (E) Bar chart showing the cell clusters as percentage component of disease. (F) Dot plot showing
 171 the representative marker genes for each subcluster. The color scale represents the scaled expression of the gene. The
 172 size of the dot represents the percentage of cells expressing the gene of interest. (I) Representative
 173 immunofluorescence of HLA-DR and CD31 in HS lesional skin. (H-I) Bar chart showing enriched Gene Ontology
 174 Biological Processes in subcluster 4 (H) and 5 (I), green; immune associated BP, orange; migration associated BP,
 175 blue; transcription/protein translation associated and other BPs.



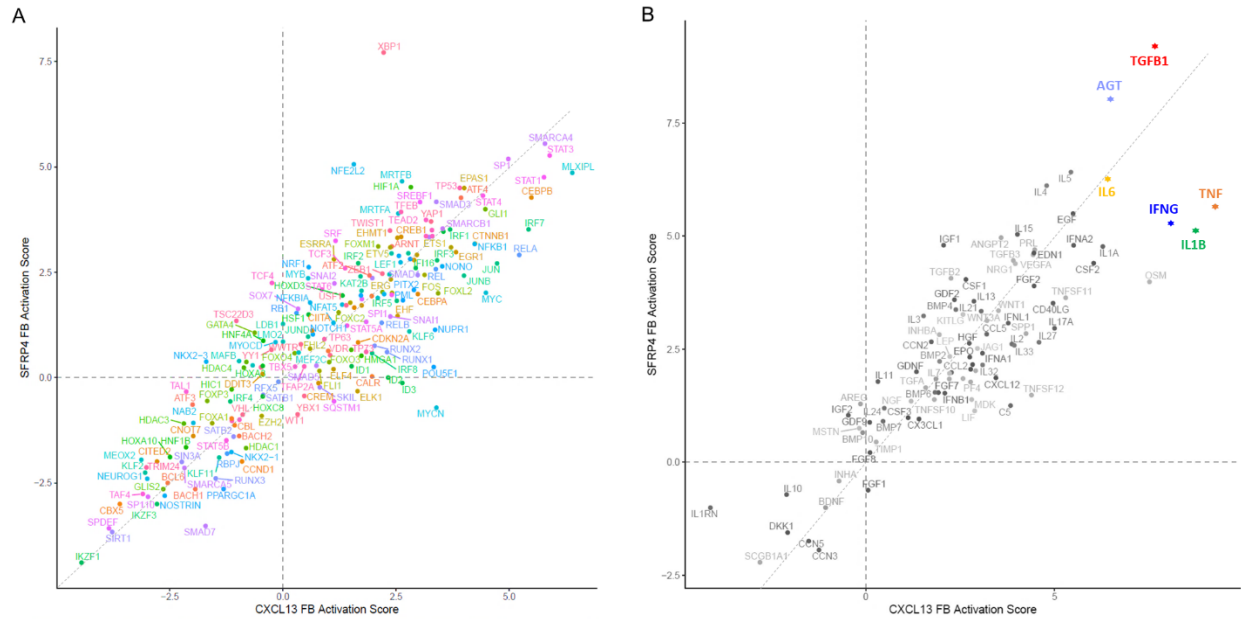
176 **Figure S6. Immunologically active vascular smooth muscle cell proliferation in HS lesional skin.**
 177 (A) UMAP plot showing 1,607 smooth muscle cells cells colored by subcluster. (B) UMAP plot showing the cells
 178 colored by disease conditions. HS: hidradenitis suppurativa; NS: normal/healthy skin. (C) Bar chart showing the cell
 179 clusters as percentage component of disease. (D) Dot plot showing the representative marker genes for each subcluster.
 180 The color scale represents the scaled expression of the gene. The size of the dot represents the percentage of cells
 181 expressing the gene of interest. (E) Bar chart showing enriched Gene Ontology Biological Processes in subcluster 0
 182 and 6 (F); green; immune associated BP, orange; angiogenesis associated BP, blue; transcription associated and other
 183 BPs.



184 **Figure S7. Expression patterns of HS primary fibroblasts.**
 185 Expression of fibroblast subtype marker genes among primary HS fibroblasts (n=5) and healthy control fibroblasts
 186 (n=3), normalized over *ACTB*; mean \pm SD; unpaired T test/Mann-Whitney U test.

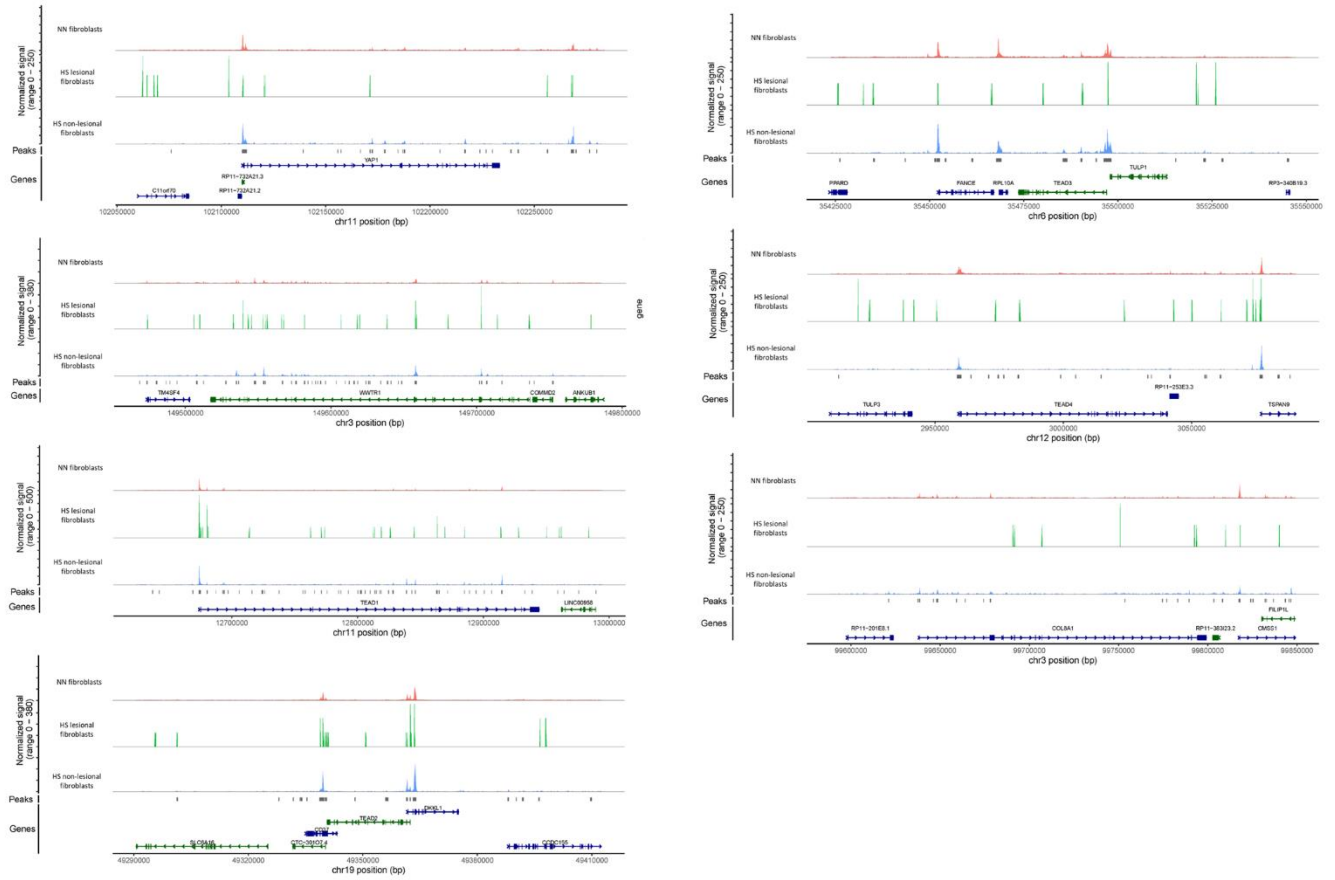


187 **Figure S8. Biological functions and activation of *SFRP4*⁺ and *CXCL13*⁺ fibroblasts.**
 188 **(A)** UMAP plots and violin plots **(B)** showing the expression level of different collagen genes in fibroblasts. **(C)** Bar chart showing the top 15 enriched biological processes among *SFRP4*⁺ fibroblasts; green; immune associated BP, orange; extracellular matrix associated BP, blue; transcription associated and other BPs. **(D)** Dot plot showing the top 30 canonical pathways enriched in *SFRP4*⁺ and *CXCL13*⁺ **(E)** fibroblasts. **(F)** Bar chart showing the top 15 enriched biological processes among *CXCL13*⁺ fibroblasts; green; immune associated BP, blue; transcription associated and other BPs.



189 **Figure S9. Activation of *SFRP4*⁺ and *CXCL13*⁺ fibroblasts.**

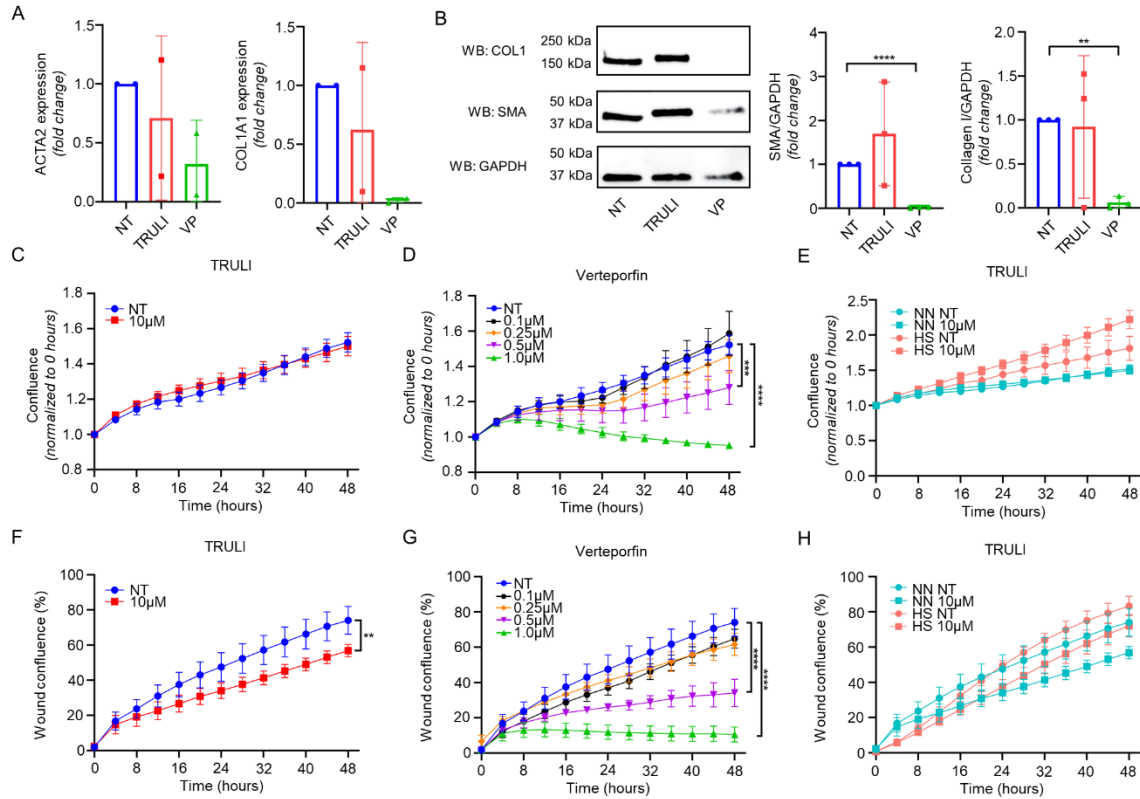
190 **(A)** Scatter plot showing the activation z scores of activated transcription factor upstream regulators for the *SFRP4*⁺
 191 and *CXCL13*⁺ FBs. **(B)** Scatter plot showing the activation z scores of activated cytokine and growth factor upstream
 192 regulators for the *SFRP4*⁺ and *CXCL13*⁺ FBs.



193
194
195
196
197
198
199
200
201

Figure S10. ATAC-seq of healthy and HS fibroblasts.

Figure showing increased chromatin accessibility as seen in the signal tracks and peaks for YAP1, WWTR1, TEAD1-4, and COL8A1 regions among HS lesional fibroblasts compared with both healthy and non-lesional HS fibroblasts. Data was obtained by performing ATAC-seq (assay of transposase accessible chromatin sequencing) on nuclei suspensions of chronic lesional and non-lesional HS skin samples of 5 patients and healthy skin from 5 controls. After quality check and alignment, peak calling was performed for YAP1, WWTR1, TEAD1-4, and COL8A1 using xxx to identify the chromatin accessibility of these regions.



202

203 **Figure S11. Modulation of the Hippo pathway in primary healthy fibroblasts.**

204 (A) Quantitative PCR results showing the effect of TRULI (T10) or verteporfin (V10, both 10 μM) on ACTA2 and
 205 COL1A1 in healthy fibroblasts. N=2. (B) Effect of TRULI or verteporfin (both 10 μM) on SMA and COL1 protein
 206 levels in healthy fibroblasts by western blotting. Data normalized to NT. n=3; **p<0.01; **** p<0.0001, mean ± SD;
 207 . (C) TRULI showed not significant increase in cell proliferation while verteporfin (D) dose-dependently blocked cell
 208 growth among healthy fibroblasts (n=2, ****p<0.0001; mean ± SEM, two-way repeated measures ANOVA). Same
 209 NT groups shown in panels C/D. (E) HS fibroblast show greater proliferation potential compared with fibroblasts,
 210 which can be further induced by treatment with TRULI. (F) treatment with TRULI did not increase healthy fibroblast
 211 migration, where verteporfin (G) showed a dose-dependent reduction in cell migration (n=2, **p<0.01,
 212 ****p<0.0001; mean ± SEM, two-way repeated measures ANOVA). Same NT groups shown in panels F/G. (H) HS
 213 fibroblasts show greater cell migration at 48 hours compared with healthy fibroblasts, however TRULI does not further
 214 increase migration of either HS or healthy cells.